

10<sup>th</sup> U. S. National Combustion Meeting  
Organized by the Eastern States Section of the Combustion Institute  
April 23-26, 2017  
College Park, Maryland

## Soot and Spectral Radiation Modeling for a High-Pressure Turbulent Spray Flame

*S. Ferreyro Fernandez<sup>1,\*</sup>, C. Paul<sup>1</sup>, A. Sircar<sup>1</sup>, A. Imren<sup>1</sup>, D. C. Haworth<sup>1</sup>, S. Roy<sup>2</sup>,  
M. F. Modest<sup>3</sup>*

<sup>1</sup>*Mechanical and Nuclear Engineering Department, The Pennsylvania State University,  
University Park, PA, USA*

<sup>2</sup>*Department of Mechanical Engineering, Marquette University, Milwaukee, WI, USA*

<sup>3</sup>*School of Engineering, University of California, Merced, CA, USA*

*\*Corresponding Author Email: suf157@psu.edu*

**Abstract:** Simulations are performed of a transient high-pressure turbulent n-dodecane spray flame under engine-relevant conditions. An unsteady RANS formulation is used, with detailed chemistry, a semi-empirical two-equation soot model, and a particle-based transported composition probability density function (PDF) method to account for unresolved turbulent fluctuations in composition and temperature. Results from the PDF model are compared with those from a locally well-stirred reactor (WSR) model to quantify the effects of turbulence-chemistry-soot interactions. Computed liquid and vapor penetration versus time, ignition delay, and flame lift-off height are in good agreement with experiment, and relatively small differences are seen between the WSR and PDF models for these global quantities. Computed soot levels and spatial soot distributions from the WSR and PDF models show large differences, with PDF results being in better agreement with experimental measurements. An uncoupled photon Monte Carlo method with line-by-line spectral resolution is used to compute the spectral intensity distribution of the radiation leaving the flame. This provides new insight into the relative importance of molecular gas radiation versus soot radiation, and the importance of turbulent fluctuations on radiative heat transfer.

**Keywords:** *Spray A, transported PDF, soot, radiation*

### 1. Introduction

Our society relies on compression-ignition engines for a wide range of applications such as transportation, construction, farming and electric power generation. In the last decades, regulations on engine exhaust emissions have become more restrictive. This has motivated the study of pollutants such as NO<sub>x</sub> and soot, the main component of particulate matter from hydrocarbon fuels. Advanced numerical simulations are necessary to achieve these goals: in particular, the study of spray flames under conditions specific to engines.

Simulation of high-pressure turbulent spray flames requires modeling of turbulent multi-phase flow, spray injection and vaporization, radiative and convective heat transfer, chemistry kinetics, and soot formation and oxidation. These physical and chemical processes occur over a wide range of time and length scales, making numerical modeling of high-pressure turbulent spray flame simulations as challenging as it is important. In addition, experimental

measurements are not always available for all quantities of interest as functions of space and time.

An important point in turbulent spray flame simulations is the modeling of turbulent fluctuations of temperature and composition, as pointed out in recent studies by Bhattacharjee and Haworth [1], Pei et al. [2] and Bolla et al. [3]. In these studies, simulations that properly account for turbulence-chemistry interactions (TCI) produced more realistic flames. Accurate temperature and species concentrations fields are essential when computing soot quantities. Soot formation and oxidation strongly depend on temperature and minor species such as poly-cyclic aromatic hydrocarbons (PAHs),  $C_2H_2$  and OH; therefore, reliable soot predictions require accounting for TCI, and also proper chemical kinetic and heat transfer models.

In general, including radiative heat transfer in numerical simulations leads to a more accurate temperature prediction and to smoother temperature fields [4]. The main sources of radiative heat loss in engines are the burned gasses and soot particles. Heywood indicates in [5] that radiation from soot particles in diesel engines is about five times larger than radiation from the burned gases. However, soot levels in modern engines have decreased significantly compared with 30 years ago, while operating pressures and exhaust gas recirculation (EGR) levels have increased, which are expected to increase the relative importance of molecular gas radiation. Recent measurements of soot radiation from spray flames under engine-relevant conditions [6] have indicated radiant fractions lower than 0.5%.

In this paper, an n-dodecane spray flame denoted by the Engine Combustion Network (ECN) as "Spray-A" is studied. The objectives of this paper are: to confirm the role of TCI in high pressure turbulent spray flames; to demonstrate the importance of molecular mixing on soot predictions; to study the effects of turbulence radiation interactions (TRI) in radiative heat transfer; and to analyze the relative contributions of participating molecular gas species and soot in the radiative heat transfer.

## 2. Methods / Experimental

The experimental configuration is a constant-volume optically accessible cubic combustion vessel with an enclosed volume of  $1147\text{ cm}^3$ . Sprays of n-dodecane ( $C_{12}H_{26}$ ) are injected using a common-rail diesel fuel injector with a single orifice of nominal diameter  $90\text{ }\mu\text{m}$  located at the center of one vessel wall. The pre-injection conditions are generated by burning a combustible mixture. Further description of the experimental set up can be found in [7].

Unsteady Reynolds-averaged simulations (URANS) of the spray injection events were performed using the open source CFD code OpenFOAM [8]. A finite-volume method was used to solve the transport equations for mean quantities. Turbulence was modeled using a standard two equation  $k-\epsilon$  model. Standard values of the turbulence model constants were used [9], except for  $C_{\epsilon 1}$  in the modeled  $\epsilon$  equation; here the value  $C_{\epsilon 1} = 1.55$  was used

The fuel injection and spray evolution were modeled using a stochastic Lagrangian parcel method [10]. In this method the spray is represented by a finite number of parcels. Liquid and gas phases were coupled by introducing source terms in mass, species, momentum and energy transport equations.

## Sub Topic: Internal Combustion and Gas Turbines

A skeletal chemical mechanism with 54 species and 269 reactions was adopted in this work [11]. This mechanism showed good agreement in previous Spray-A simulations for ignition delay and lift-off [11], [12].

The effects of turbulent fluctuations in species composition, soot quantities and enthalpy were explicitly accounted using a transported PDF method. The composition variables were taken to be the mass fractions of the  $N_s$  species in the chemical mechanism, the  $N_{SOOT}$  quantities from the soot model, and the mixture-specific absolute enthalpy. A Lagrangian Monte Carlo approach was used to solve the PDF transport equation. PDF simulations are compared with a locally well stirred reactor (WSR) model, which neglects turbulent fluctuations.

Turbulent transport was modeled using the gradient-diffusion assumption. The Euclidean Minimum Spanning Tree (EMST) model [13] was employed to represent molecular mixing. All the required information about the turbulence scales is calculated by the finite volume flow solver using the  $k$ - $\epsilon$  model. Detailed information of the modeled PDF equation, the corresponding particle equations, and mixing models can be found in [14] and references therein.

A semi-empirical two-equation soot model proposed in [15] was used to predict soot volume fraction and average soot number density. In this model, inception is based on acetylene, which makes it suitable for reduced chemical mechanisms without PAHs. Soot oxidation paths were augmented with the two reactions suggested in [16].

Radiative heat transfer was computed using a Photon Monte Carlo (PMC) method [17]. The participating gases considered here are  $CO_2$ ,  $H_2O$  and  $CO$ . Spectral properties were obtained from the HITEM 2010 database. Soot spectral properties follow the correlation given in [18].

The computational domain is a 2-D axisymmetric mesh that represents a  $5^\circ$  section of the entire vessel. The axial  $z$  and radial  $r$  extents of the domain are 108 mm and 58 mm, respectively. The radial extent was selected to ensure consistency between the computational domain and experimental vessel volumes.

The mesh consists of 12,800 nonuniformly distributed hexahedral cells, with higher resolution close to the fuel injector orifice. The minimum characteristic cell dimension is 0.25 mm. Symmetry conditions were applied at all boundaries, except along solid walls where zero velocity and standard wall functions were applied. All simulations were performed with a computational time step of 0.5  $\mu$ s. The number of stochastic particles per cell for PDF runs was maintained between 50 and 100.

The baseline initial temperature, pressure and density in the vessel are 900 K, 60 bar, and 22.8 kg/m<sup>3</sup>. The non-reacting case has an  $O_2$  molar concentration of 0%, and uses nozzle 210677. Reacting cases have an  $O_2$  molar concentration of 15% and use nozzle 210370. The nominal fuel injection pressure is 150 MPa and the total injection duration is 6 ms.

### 3. Results and Discussion

Non-reacting experimental data obtained at Sandia National Laboratories include liquid and vapor penetration, and mixture fraction spatial distributions. Detailed explanation of the experimental measurements can be found in [7] and [19]. Initial turbulence kinetic energy, turbulence dissipation rate and spray parameters were adjusted to match the experimentally measured penetrations and mixture fraction distributions. There are small differences between WSR and PDF results for the non-reacting case.

Reacting cases are simulated next. First, two main key quantities were computed and compared with the experimental measurements: the ignition delay and the lift-off length (Figure 1). Ignition delays for WSR and PDF models are similar, and both are somewhat lower than the experimental measurements.

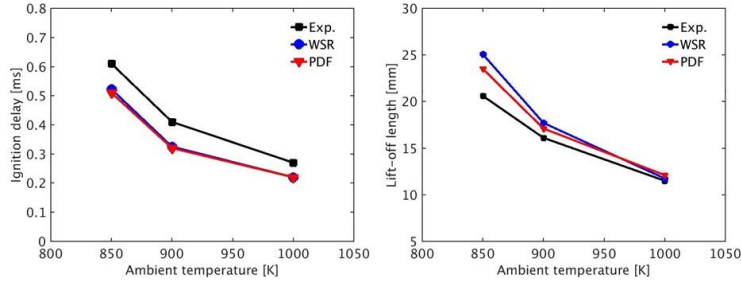


Figure 1: Computed and measured ignition delays (left) and lift-off lengths (right) as functions of ambient temperature.

On the other hand, PDF model lift-off lengths are somewhat better compared to WSR at temperatures below 900 K. Similar results were showed in [1] and [2]. At high temperatures, computed lift-off lengths for both models are essentially the same, and are in good agreement with experiment.

Available soot experimental data includes quantitative measurements of soot optical thickness (KL) performed using laser extinction and planar laser-induced incandescence (PLII). The experimental setup is reported in [20], and measurements are available for ambient temperatures of 850 K, 900 K and 1000 K. These measurements cover a large region of the flame that extends from 15.2 mm to 67.2 mm from the fuel nozzle. The soot optical thickness can then be related to soot quantities such as soot volume or mass fractions [21].

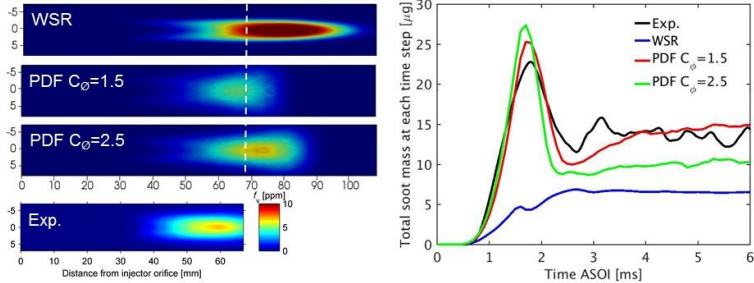


Figure 2. Left: Computed and measured time-averaged soot volume fraction contours. Right: Computed and measured total soot mass in the experimental field of view.

In Figure 2 (left), computed averaged soot volume fraction contours are compared with experimental measurements from the ECN database. The key feature is the spatial distribution of soot. The soot cloud location and distribution from the PDF simulation is closer to the experimental measurements than are those from the WSR simulation. In addition, the peak soot volume fraction from the PDF model with  $C_\phi=1.5$  (4 ppm) is much smaller than the peak predicted by the WSR model (16 ppm), with the PDF model value being closer to the peak experimentally measured value (7 ppm).

The influence of mixing can also be seen in **Figure 2 (right)**. Computed total soot mass from the PDF simulation for two values of the mixing model coefficient  $C_\phi$  are presented. The most important feature of the PDF model is that it is able to capture the transient shape of the total

## Sub Topic: Internal Combustion and Gas Turbines

soot mass versus time. WSR simulations fail to capture the early rapid rise and peak/falloff at approximately 2 ms. Increasing the mixing rate leads to higher total soot mass, with the soot cloud further downstream.

Results from PMC/LBL radiation post-processing are presented in Table 1. There the analysis considers only flame zone radiation, where the flame zone is defined as any cell with a temperature above 1000 K.  $\text{CO}_2$  dominates the radiative emission. However, most of the radiative energy emitted by  $\text{CO}_2$  is reabsorbed and only about a 5% leaves the flame. This analysis reveals that  $\text{CO}_2$  contributes to a redistribution of energy rather than to heat loss out of the flame. Therefore,  $\text{CO}_2$  radiation produces more uniform temperature fields.

On the other hand,  $\text{H}_2\text{O}$  dominates the radiative energy that reaches the wall, accounting for more than half of the total. The effects of TRI are stronger for soot radiation than for molecular gas radiation. This suggests that when studying soot radiation, TRI should be taken into account when comparing with experimental measurements, i.e. the spectral and spatial radiative intensities presented in [6].

Radiation Source	Participating Quantity	Energy Emitted		Energy Reabsorbed		Energy out of the flame	
		(W)	(%)	(W)	(%)	(W)	(%)
Cell level	$\text{CO}_2$	29.35	82.34	27.82	91.00	1.54	30.25
	$\text{H}_2\text{O}$	5.37	15.07	2.55	8.35	2.82	55.54
	CO	0.19	0.54	0.12	0.40	0.07	1.40
	Soot	0.73	2.04	0.08	0.25	0.65	12.80
Particle level	$\text{CO}_2$	31.96	78.95	29.47	90.32	2.50	31.79
	$\text{H}_2\text{O}$	6.42	15.87	2.85	8.74	3.57	45.44
	CO	0.22	0.55	0.14	0.44	0.08	0.98
	Soot	1.88	4.63	0.16	0.50	1.71	21.79

Table 1: Radiative contributions from key participating constituents from PMC/LBL postprocessing. Results are at 4.0 ms ASOI, for a PDF  $C_\phi=1.5$  run.

## 4. Conclusions

Simulations of transient high-pressure turbulent n-dodecane spray flames under engine-relevant conditions were performed. An unsteady RANS formulation was used, with detailed chemistry, a semi-empirical two-equation soot model, and, a transported PDF method to account for unresolved turbulent fluctuations in composition and temperature.

Results from the PDF model were compared with those from a WSR model to quantify the effects of turbulence-chemistry-soot interactions. Computed liquid and vapor penetration versus time, ignition delay, and flame lift-off height were in good agreement with experiment, and relatively small differences are seen between the WSR and PDF models for these global quantities.

Computed soot levels and spatial soot distributions from the WSR and PDF models show large differences, with PDF results being in better agreement with experimental measurements. A photon Monte Carlo method with line-by-line spectral resolution is used to compute the spectral intensity distribution of the radiation that reaches the wall. It was found that gas emission is dominated by  $\text{CO}_2$  and the radiative heat loss by  $\text{H}_2\text{O}$ . The influence of turbulent fluctuations is most apparent in soot radiation.

## 5. Acknowledgements

This material is based upon work supported by the Department of Energy, Office of Energy Efficiency and Renewable Energy (EERE) and the Department of Defense, Tank and Automotive Research, Development, and Engineering Center (TARDEC), under Award Number DE-EE0007278.

## 6. References

- [1] S. Bhattacharjee, D.C. Haworth, Simulations of transient n-heptane and n-dodecane spray flames under engine-relevant conditions using a transported PDF method, *Combustion and Flame* 160 (2013) 2083-2102.
- [2] Y. Pei, E.R. Hawkes, S. Kook, G.M. Goldin, T. Lu, Modelling n-dodecane spray and combustion with the transported probability density function method, *Combustion and Flame* 162 (2015) 2006-2019.
- [3] M. Bolla, M.A. Chishty, E.R. Hawkes, Q.N. Chan, S. Kook, Influence of turbulent fluctuations on radiation heat transfer, NO and soot formation under ECN Spray A conditions, *Proceedings of the Combustion Institute* 36 (2017) 3551–3558.
- [4] P.J. Coelho, Numerical simulation of the interaction between turbulence and radiation in reactive flows, *Progress in Energy and Combustion Science* 33 (2007) 311-383.
- [5] J.B. Heywood, *Internal Combustion Engine Fundamentals*, McGraw-Hill Edition 1988.
- [6] S. Skeen, J. Manin, L. Pickett, Quantitative spatially resolved measurements of total radiation in high-pressure spray flames, 2014.
- [7] L.M. Pickett, L.G. Genzale, G. Bruneaux, L.-M. Malbec, L. Hermant, C. Christiansen, J. Schramm, Comparison of Diesel Spray Combustion in Different High-Temperature, High-Pressure Facilities, *SAE Int. J. Engines* 3(2) (2010).
- [8] OpenFOAM: The Open Source CFD Toolbox. <http://www.openfoam.org>.
- [9] B.E. Launder, D.B. Spalding, The numerical computation of turbulent flows, *Comput. Methods Appl. Mech. Eng.* 3 (1973) 269--289.
- [10] J.K. Dukowicz, A particle-fluid numerical model for liquid sprays, *Journal Combustion and Physics* 35 (1980) 229-253.
- [11] T. Yao, Y. Pei, B.-J. Zhong, S. Som, T. Lu, A hybrid mechanism for n-dodecane combustion with optimized low-temperature chemistry, 9th U.S. National Combustion Meeting, Cincinnati, Ohio, USA, 2015.
- [12] S. Skeen, J. Manin, L. Pickett, E. Cenker, et al., A progress review on soot experiments and modeling in the Engine Combustion Network (ECN), *SAE International Journal of Engines* 9 (2016).
- [13] S. Subramaniam, S. B. Pope, A mixing model for turbulent reactive flows based on Euclidean Minimum Spanning Trees, *Combustion and Flame* 115 (1998) 487-514.
- [14] D.C. Haworth, Progress in probability density function methods for turbulent reacting flows, *Progress in Energy and Combustion Science* 36 (2010) 168-259.
- [15] K.M. Leung, R.P. Lindstedt, W.P. Jones, A simplified reaction mechanism for soot formation in nonpremixed flames, *Combustion and Flame* 87 (1991) 289-305.
- [16] H. Guo, F. Liu, G.J. Smallwood, Soot and NO Formation in Counterflow Ethylene/Oxygen/Nitrogen Diffusion Flames, *Combustion Theory and Modeling* 8 (1991) 475-489.
- [17] M.F. Modest, *Radiative Heat Transfer*, Second edition ed., Academic Press, New York, 2003.
- [18] H. Chang, T. Charalampopoulos, Determination of the wavelength dependence of refractive indices of flame soot, *Proceedings of the Royal Society* 430 (1990) 557-591.
- [19] L.M. Pickett, J. Manin, C.L. Genzale, D.L. Siebers, M.P.B. Musculus, C.A. Idicheria, Relationship Between Diesel Fuel Spray Vapor Penetration/Dispersion and Local Fuel Mixture Fraction, *SAE Int. J. Engines* 4(1) (2011) 764-799.
- [20] M.P.B. Musculus, L.M. Pickett, Diagnostic considerations for optical laser-extinction measurements of soot in high-pressure transient combustion environments, *Combustion and Flame* 141 (2005) 371–391.
- [21] L.M. Pickett, D.L. Siebers, Soot in diesel fuel jets: effects of ambient temperature, ambient density, and injection pressure, *Combustion and Flame* 138 (2004) 114-135.